Catal Lett (2009) 129:135–141
DOI 10.1007/s10562-008-9799-4

Significant Improvement in Activity and Stability of Pt/TiO_2 Catalyst for Water Gas Shift Reaction Via Controlling the Amount of Na Addition

Xinli Zhu · Trung Hoang · Lance L. Lobban · Richard G. Mallinson

Received: 16 October 2008 / Accepted: 21 November 2008 / Published online: 4 December 2008

Abstract Na promoted Pt/TiO_2 catalysts have been studied under high severity, near equilibrium, conditions for use as a single stage WGS catalyst. Addition of 3 wt% Na to a 1 wt% Pt/TiO_2 catalyst has been found to improve water gas shift activity significantly compared to Pt/TiO_2, Pt/CeO_2, and $Pt–Re/TiO_2$ catalysts. This catalyst is stable when the reaction temperature is higher than 250 °C. Deactivation occurred when the reaction temperature was lower than 250 °C, however, returning the temperature to higher than 250 °C fully recovered activity. TEM observations revealed that addition of Na inhibited Pt particle sintering. These results suggest that Na promoted Pt/TiO_2 is a promising single stage water gas shift catalyst for small scale hydrogen production.

Keywords Water gas shift · Sodium · Pt/TiO_2 · Hydrogen

1 Introduction

The water gas shift (WGS) reaction is a crucial step to remove CO and produce additional H_2 from synthesis gas obtained from reforming of hydrocarbon or oxygenated hydrocarbon fuels:

$$CO + H_2O \leftrightarrow CO_2 + H_2, \quad \Delta H = -41.2\,\mathrm{kJ/mol}.$$

The industrial WGS process is the well developed two-step shift: Fe/Cr based high temperature shift and Cu–Zn–Al based low temperature shift. This process can successfully reduce CO to lower than 4000 ppm [1]. Because the Cu based catalyst is pyrophoric and needs a very careful activation process, it cannot easily meet the strict requirements for onboard or small scale hydrogen production for polymer electrolyte fuel cells [1], that have a much higher efficiency than internal combustion engines. Therefore, noble metal based catalysts, especially Pt based catalysts, have received much attention for this application.

Extensive studies have focused on the highly active Pt/CeO_2 catalyst for the reaction mechanisms: associate mechanism or redox (regenerate) mechanism [2–5]. In both reaction mechanisms, CO is adsorbed on Pt particles and H_2O is activated on the support. Thus both the supported metal and support play important roles in the activity and stability of the catalyst for WGS. However, deactivation of the Pt/CeO_2 catalyst under working conditions (both long time runs at certain temperatures and shutdown-startup cycles) is usually observed. Deactivation due to over-reduction of the CeO_2 support, surface carbonate (stable up to 430 °C) and/or formate formation as well as Pt sintering have been suggested [6–8]. Note that both over-reduction of CeO_2 and the consequent formation of surface carbonate (and possibly cerium (III) hydrocarbonate [9]) are related to the intrinsic properties of the high reducibility of nano-sized CeO_2 particles in the presence of noble metals, such as Pt, Pd, Rh, etc. This presents a difficult problem because it is determined by the support properties. Some efforts have been made to overcome this problem: addition of small amounts of O_2 to the feed to inhibit the formation of surface carbonate [9] and addition of ZrO_2 to CeO_2 to improve the support properties [8].

Some less reducible supports, such as TiO_2 and ZrO_2, are possible alternatives to CeO_2. Pt/ZrO_2 is stable for the WGS reaction, but its activity is much lower than Pt/CeO_2 [10], even though significant improvement has been

X. Zhu · T. Hoang · L. L. Lobban · R. G. Mallinson (✉)
School of Chemical, Biological, and Materials Engineering, The University of Oklahoma, Norman, OK 73019, USA
e-mail: mallinson@ou.edu

achieved by addition of alkali metals [11]. Increasing attention has been paid to Pt/TiO_2 catalysts for WGS, because it shows similar or greater activity compared to Pt/CeO_2 [10, 12–17]. However, in contrast to the Pt/CeO_2 catalyst, deactivation due to Pt sintering at high temperatures during the WGS reaction has been observed for Pt/TiO_2 catalysts [10]. Addition of Re to the Pt/TiO_2 inhibits this deactivation and improves the activity for the WGS reaction [10, 15–17]. In order to meet the requirement of high space velocity operation to reduce the reactor volume for onboard and small scale H_2 production, further increases in both activity and stability of the Pt/TiO_2 are highly desired.

This work shows that controlling the amount of Na addition to the Pt/TiO_2 catalyst can lead to significant improvement in the activity and stability for WGS under high severity, equilibrium, conversion. Two well studied catalysts, Pt/CeO_2 and $Pt–Re/TiO_2$, were also included for comparison.

2 Experimental

2.1 Catalyst Preparation

The sodium promoted Pt/TiO_2 catalysts were prepared by incipient wetness impregnation of TiO_2 (Degussa P25, BET surface area 49 m^2/g) with aqueous $NaNO_3$ (Aldrich) and $H_2PtCl_6 \cdot 6H_2O$ (Aldrich) at the same time. The Pt loading was fixed as 1 wt%. The amount of sodium loading was varied from 0 to 10%. The resulting samples were dried at 110 °C for 12 h and finally calcined in flowing air at 400 °C for 4 h. These samples are denoted as Pt–xNa, where x is the percentage of sodium loading.

For the Re promoted Pt/TiO_2 catalyst, the TiO_2 (Degussa P25) powder was impregnated for 1 h with NH_4ReO_4 (Aldrich) solution, then impregnated with $H_2PtCl_6 \cdot 6H_2O$ (Aldrich) solution for another 12 h [10]. The resulting sample was dried at 110 °C for 12 h and then was calcined in flowing air at 400 °C for 4 h. Both Pt and Re loadings are 1 wt%.

The CeO_2 was prepared via homogeneous precipitation of ceria nitrate in urea with aqueous ammonia [3, 18, 19]. For preparation of 6 g of CeO_2, 14.7535 g $Ce(NO_3)_3 \cdot 6H_2O$ (Aldrich) and 48 g urea (Aldrich) were dissolved in 180 mL deionized water. 6 mL $NH_3 \cdot H_2O$ was added dropwise to the solution while stirring. The resultant mixture was boiled at 100 °C for 8 h, and then filtered and washed with hot water twice. The sample obtained was dried at 110 °C for 12 h and finally calcined in air at 400 °C for 4 h. 1 wt% Pt was introduced to the CeO_2 by incipient wetness impregnation of CeO_2 with aqueous $H_2PtCl_4 \cdot 6H_2O$ (Aldrich) solution at room temperature for 12 h, dried at 110 °C for 12 h and finally calcined in air at 400 °C for 4 h.

2.2 Activity Tests

The activity tests were carried out using a tubular quartz reactor at atmospheric pressure. The catalyst sample (0.2 g, 40–60 mesh) was reduced in situ at 300 °C for 1 h before reaction. H_2 was included in the feed gas because H_2 plays a significant equilibrium limiting role on the WGS reaction [20] and H_2 will be present in the WGS feed from the reformer. In this study, CO_2 was not included in the feed gas for these experiments because it plays a much smaller inhibition role than H_2 does [20] and it accumulates during these high conversion experiments. A feed containing H_2 (70 mol%) and CO (30 mol%) (on a dry basis) was introduced by mass flow controllers. H_2O was introduced by a calibrated HPLC pump. The H_2O:CO molar ratio was 5:1. For a typical run, the gas hourly space velocity (GHSV) is 1.5×10^4 cm^3/g-cat h (H_2O not included; e.g. dry basis). The gases (H_2, CO_2, CO) after reaction were online analyzed by a Carle AGC 400 gas chromatograph (with HTS hydrogen analysis system) after passing through a cold trap to remove water. No CH_4 or other hydrocarbons were detected in any experiment.

2.3 Characterizations

X-ray powder diffraction (XRD) patterns of the catalysts samples were recorded by a Bruker D8 Discover diffractometer at a scanning speed of 2°/min, with a Cu Kα radiation source ($\lambda = 1.54056$ Å). The support particle size was estimated from the full width at half maximum of diffraction peak using the Scherrer formula.

Transmission electron microscopy (TEM) observations were performed on a Philips JEOL 2000-FX system operated at 200 kV. The catalyst powder was dispersed ultrasonically in ethanol. A drop of the suspension was deposited on a carbon coated copper grid for TEM analysis. The number-weighted particle size d_n is calculated by the following formula: $d_n = \sum n_i d_i / \sum n_i$, where d_i is the particle size of n_i particle. Approximately 200 particles from different TEM photos of the sample were used to calculate the d_n.

3 Results and Discussion

The XRD pattern of CeO_2 shows the fluorite structure, with an average particle size of 11 nm estimated from CeO_2 (111). Loading of Pt onto the CeO_2 does not change the crystal phase and particle size of CeO_2. The Pt species (Pt, PtO, and PtO_2) diffraction peaks are absent in the XRD

pattern, suggesting that the Pt species are highly dispersed on the CeO_2.

The XRD pattern of TiO_2 shows a mixed structure of anatase (80%) and rutile (20%). The average particle sizes of TiO_2 are 17 nm for anatase and 23 nm for rutile. Loading of Pt, Pt–Na, and Pt–Re does not change the particle size of TiO_2. No Pt species can be observed, indicating the Pt species are highly dispersed on the TiO_2 support.

The effect of support (CeO_2 and TiO_2) and promoter (Re and Na) on the WGS reaction activity were first tested (Fig. 1). It can be seen that the Pt/TiO_2 and Pt/CeO_2 show similar activity for WGS reaction, with Pt/CeO_2 slightly more active at high reaction temperatures (>275 °C) and Pt/TiO_2 slightly more active at low reaction temperatures (<275 °C). Addition of 1 wt% Re to the Pt/TiO_2 improves the WGS activity at high reaction temperatures (>275 °C), but decreases the WGS activity at low reaction temperatures (<275 °C). Farrauto et al. also found similar results of Re promoted Pt-based catalyst for the WGS reaction [21]. The CO conversion is always increasing in the reaction temperature range of 200–350 °C over Pt/TiO_2, Pt/CeO_2, and Pt–1Re/TiO_2 catalysts, indicating that CO conversion has not reached equilibrium over these catalysts at these space velocities. Addition of 2 wt% Na to the Pt/TiO_2 catalyst significantly improves the WGS reaction activity. The CO conversion reaches 92.9% at 250 °C, and 98.1% at 275 °C, and then slowly decreases to 96.2% at 350 °C, indicating that CO reaches equilibrium at 275 °C. It has been suggested [22] that the promoting effect of Na is related to Na species modifying the electronic structure of the closely contacted Pt, weakening the C–H bond of the formate intermediate adsorbed on the Pt surface, consequently accelerating the decomposition of formate, as evidenced by infrared spectroscopy. Therefore, Na addition improves the formate mediated WGS reaction pathway, resulting in a higher CO conversion activity.

The optimal Na loading was determined by varying the Na loading and the results are shown in Fig. 2. The activity for WGS decreases in the following order: Pt–3Na > Pt–2Na > Pt–4Na > Pt–6Na > Pt–10Na > Pt > Pt–1Na. Increasing the Na loading from 2 to 3 wt% further improves the WGS reaction activity. The CO conversion is 48.7% at 200 °C, and 96.2% at 225 °C, and reaches equilibrium at 250 °C at this space velocity. Further increases in the amount of Na loading gradually decreases the WGS reaction activity, typically as a result of coverage of the Pt surface by excess Na species, decreasing the exposed Pt surface area.

Although addition of 2 wt% Na to Pt/TiO_2 significantly improves the WGS reaction activity, addition of 1 wt% Na to Pt/TiO_2 suppresses the WGS reactivity. This result is reproducible with different runs of the same batch of catalyst or experiments with different batches of catalysts.

The stability of the Pt/TiO_2, Pt–1Re/TiO_2, and Pt–3Na/TiO_2 was tested at 300 °C for 20 h (Fig. 3). This is a useful point because of the fact that hydrogen selective membranes are stable at those conditions [10]. For Pt/TiO_2, CO conversion decreases continually from 75.2% at the

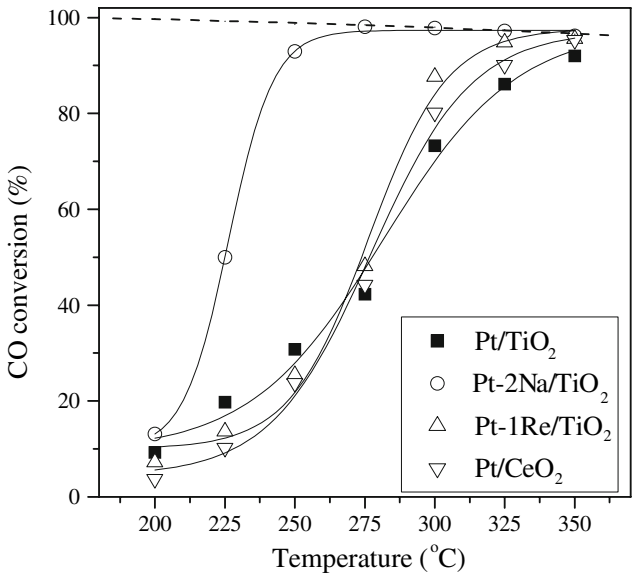

Fig. 1 Effect of support (TiO_2 and CeO_2) and promoter (Re and Na) of supported Pt catalyst on WGS activity. Dashed line is the calculated CO equilibrium conversion under the present feed condition. Reaction conditions: 70% H_2, 30%, H_2O:CO = 5:1, 0.2 g catalyst, GHSV = 1.5×10^4 cm^3/g-cat h (H_2O not included)

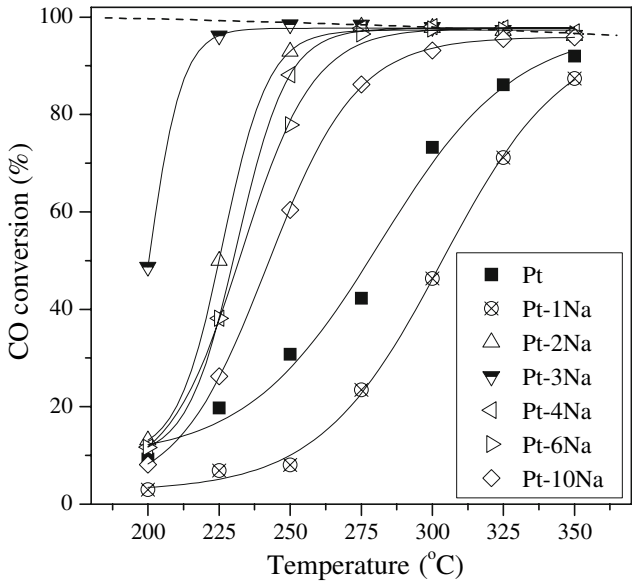

Fig. 2 Effect of the amount of Na loading of Pt/TiO_2 on the WGS activity. Dashed line is the calculated CO equilibrium conversion under the present feed condition. Reaction conditions: 70% H_2, 30%, H_2O:CO = 5:1, 0.2 g catalyst, GHSV = 1.5×10^4 cm^3/g-cat h (H_2O not included)

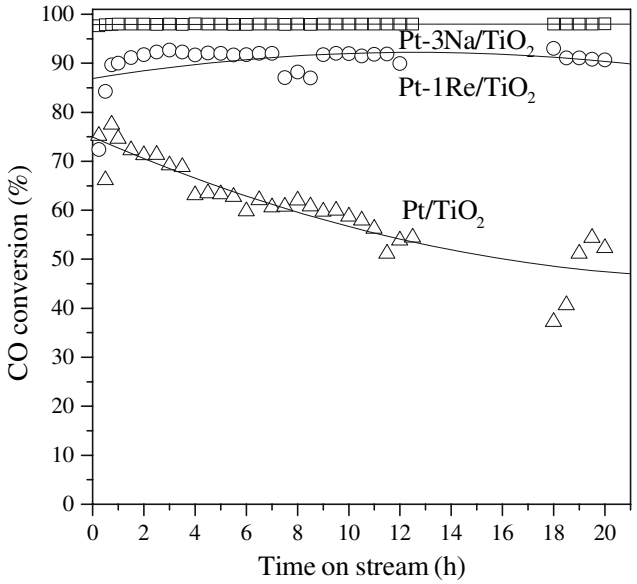

Fig. 3 Stability of Pt/TiO_2, $Pt–1Re/TiO_2$, and $Pt–3Na/TiO_2$ for WGS at 300 °C. Reaction conditions: 70% H_2, 30%, H_2O:CO = 5:1, 0.2 g catalyst, GHSV = 1.5×10^4 cm^3/g-cat h (H_2O not included)

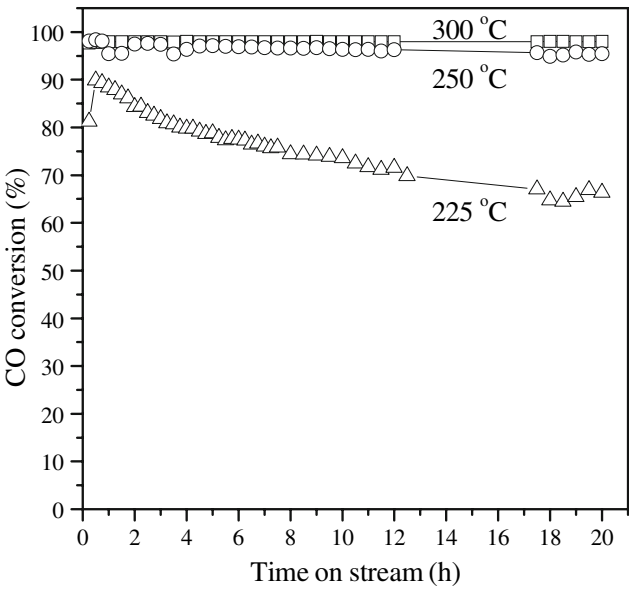

Fig. 4 Stability tests of $Pt–3Na/TiO_2$ for WGS reaction at 300, 250, and 225 °C. Reaction conditions: 70% H_2, 30%, H_2O:CO = 5:1, 0.2 g catalyst, GHSV = 1.5×10^4 cm^3/g-cat h (H_2O not included)

beginning of reaction to 52.3% at the end of 20 h run. For $Pt–Re/TiO_2$, CO conversion stabilized at 91% over 20 h time on steam. These results are in agreement with Azzam at el [10]. For $Pt–3Na/TiO_2$, CO conversion is 97.8% without any observable deactivation during 20 h time on stream.

$Pt–3Na/TiO_2$ was further tested at 250 and 225 °C to check the effect of reaction temperature on its stability (Fig. 4). Slight deactivation is observed at 250 °C with CO conversion stabilized at approximately 96% by the end of the 20 h run. Obvious deactivation is observed for the reaction temperature of 225 °C, with a CO conversion of 66.4% at the end of the 20 h run. These results indicate that the $Pt–3Na/TiO_2$ is stable when the reaction temperature is higher than 250 °C. The deactivation at lower reaction temperature is may be related to the build up of surface formate and/or carbonate species that hinder the reaction [9].

Another stability test of $Pt–3Na/TiO_2$ was made by increasing the reaction temperature stepwise from 200 to 225 °C, and finally to 250 °C (Fig. 5). It can be seen that the catalyst showed deactivation at reaction temperatures of 200 and 225 °C, however the CO conversion is stabilized at about 95% when the temperature is finally increased to 250 °C. This is almost the same CO conversion as in the stability test that was performed at 250 °C for 20 h (Fig. 4), indicating that the catalyst activity fully recovered at 250 °C even though it deactivated at 200 and 225 °C. This result again supports the idea that the catalyst is stable when the reaction temperature is higher than 250 °C. This result also indicates that the deactivation of the catalyst at low reaction temperatures (<250 °C) is

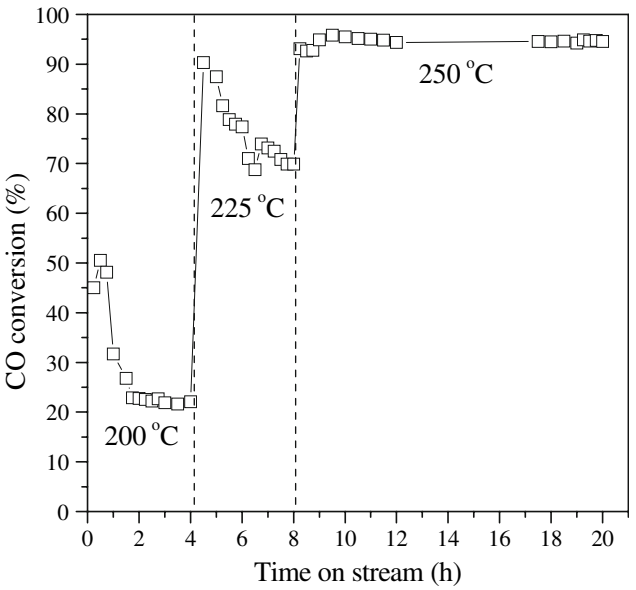

Fig. 5 Effect of reaction temperature on the stability of $Pt–3Na/TiO_2$ for WGS reaction. Reaction conditions: 70% H_2, 30%, H_2O:CO = 5:1, 0.2 g catalyst, GHSV = 1.5×10^4 cm^3/g-cat h (H_2O not included)

reversible, i.e. the formation of inert surface carbonate and/or formate; not irreversible.

TEM observations were carried out to evaluate the Pt particle size changes before and after 20 h WGS run at 300 °C, and the results are shown in Fig. 6. An obvious increase in Pt particle size from 1.4 to 2.0 nm is observed for Pt/TiO_2 after 20 h of WGS reaction (Fig.6a, b), indicating that the deactivation of Pt/TiO_2 is due to Pt

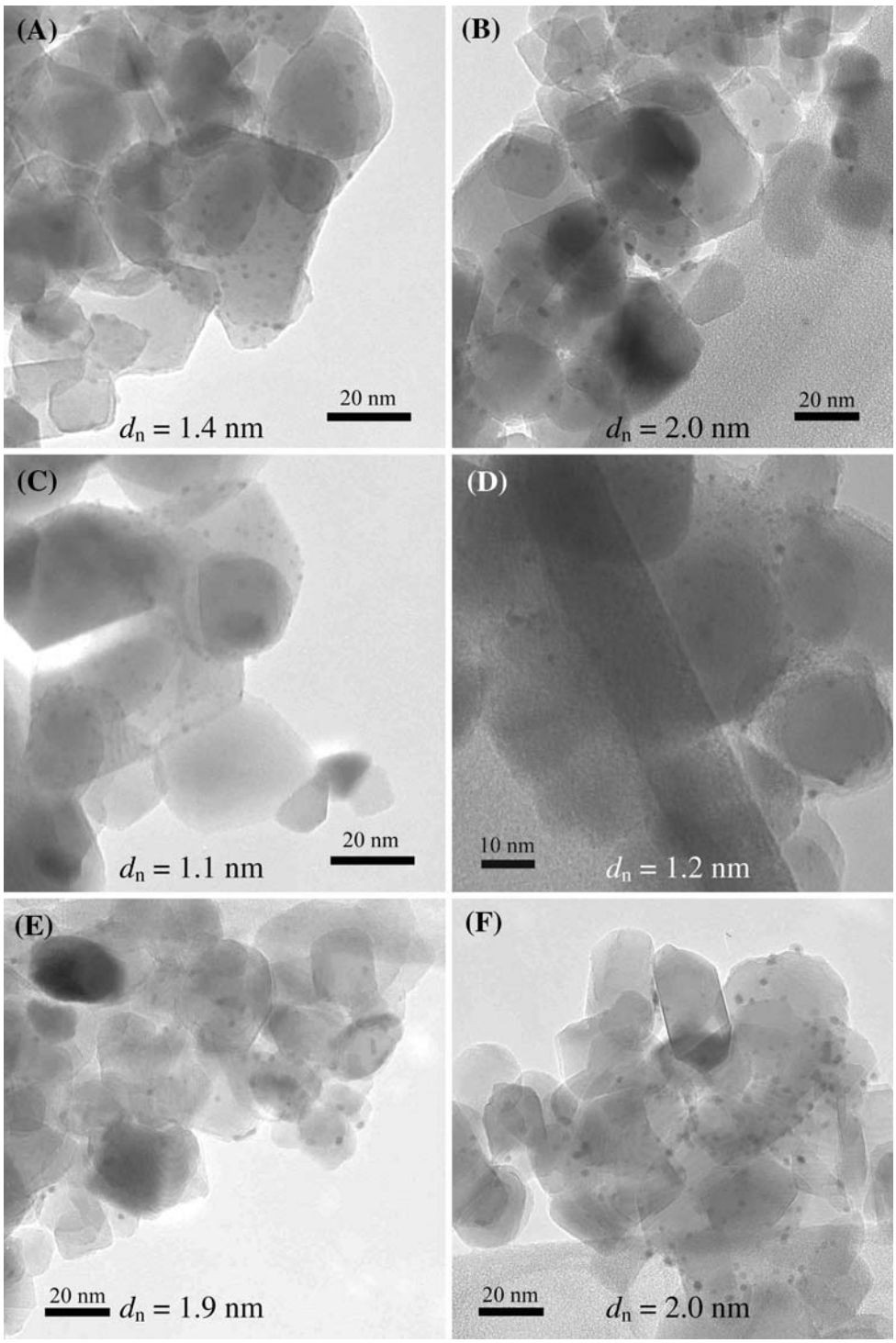

Fig. 6 TEM images of freshly reduced Pt/TiO_2 (**a**), Pt–1Re/TiO_2 (**c**), Pt–3Na/TiO_2 (**e**); and used Pt/TiO_2 (**b**), Pt–1Re/TiO_2 (**d**), Pt–3Na/TiO_2 (**f**) for WGS reaction at 300 °C for 20 h

sintering. Addition of 1 wt% Re to the Pt/TiO_2 decreases the particle size (Fig. 6c, $d_n = 1.1$ nm). After 20 h WGS reaction, no Pt sintering is observed (Fig. 6d, $d_n = 1.2$ nm). These results are in good agreement with Azzam et al. [10].

The particle size is 1.9 nm for freshly reduced Pt–3Na/TiO_2 catalyst and after 20 h of WGS reaction, the average particle size is 2.0 nm (Fig. 6e, f), indicating that addition of Na to Pt/TiO_2 kept Pt from sintering, possibly in the form of Pt–NaO_x–TiO_2 interactions. Since the Pt has not sintered at high reaction temperature (300 °C), the deactivation of the catalyst at lower reaction temperatures (<250 °C) should not be due to Pt sintering, but is due to the formation of surface carbonate and/or formate.

The stability test for the Pt–3Na sample was carried out at 300 °C, essentially reaching equilibrium at the chosen space velocity, which could mask deactivation of the catalyst if there is excess catalyst. The Pt–3Na sample was run using a higher GHSV of 7.0×10^4 cm^3/g-cat h to further test the stability at non-equilibrium conditions, resulting in a CO conversion lower than equilibrium, as shown in Fig. 7. Even though the GHSV is 5 times higher than the Pt/TiO_2 catalyst, the CO conversion is higher for Pt–3Na/TiO_2 than for Pt/TiO_2. Only slight deactivation is observed at the beginning of reaction. After 20 h reaction, CO conversion was stable at 85%. Additionally, startup-shutdown cycles of the Pt–3Na/TiO_2 sample with a GHSV of 7.0×10^4 cm^3/g-cat h were tested, as shown in Fig. 8. In the first shutdown, CO and H_2O were removed. In the second shutdown, only H_2O was removed. It can be seen that the CO conversion was recovered after the reaction startup again for both shutdowns, indicating the catalyst is stable under these shutdown-startup conditions.

For the Pt–3Na/TiO_2, the CO conversion reaches equilibrium in the temperature range of 250–350 °C at a GHSV of 1.5×10^4 cm^3/g-cat h. The effect of space velocity on CO conversion tests (not shown) showed that CO conversion reaches equilibrium when the GHSV is lower than 4.0×10^4 cm^3/g-cat h. Under these conditions, a single stage WGS shift using Pt–3Na/TiO_2 as catalyst can effectively remove CO from 30 to 0.52% (dry basis) with a very high space velocity. The resultant reformate after WGS can be directly processed by CO preferential oxidation to remove the residual CO for fuel cell applications. The Pt–3Na/TiO_2 catalyst is highly active and stable under high severity conditions (high space velocity, near equilibrium conversion, excess water, high CO concentration, high produced CO_2 concentration (up to ~23%, dry basis)). Therefore, Pt–3Na/TiO_2 is a promising single stage WGS catalyst.

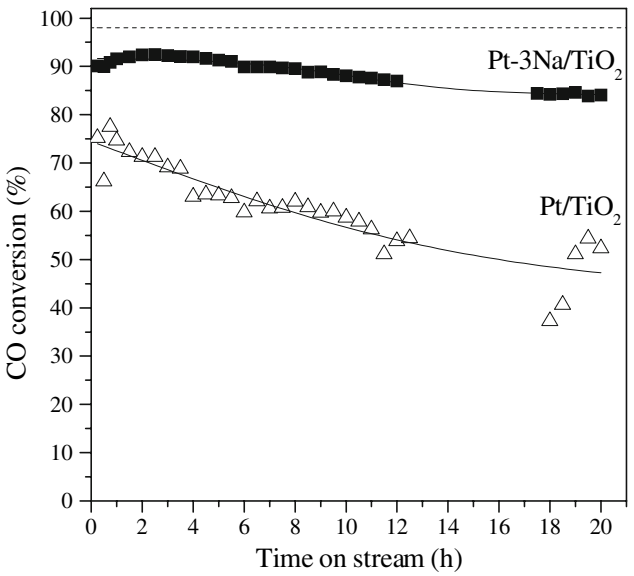

Fig. 7 Stability tests of Pt/TiO_2 and Pt–3Na/TiO_2 for WGS at 300 °C. Reaction conditions: 70% H_2, 30%, H_2O:CO = 5:1, GHSV = 7.0×10^4 cm^3/g-cat h for Pt–3Na/TiO_2, and GHSV = 1.5×10^4 cm^3/g-cat h for Pt/TiO_2 (H_2O not included). Dashed line is the calculated CO equilibrium conversion under the present feed condition

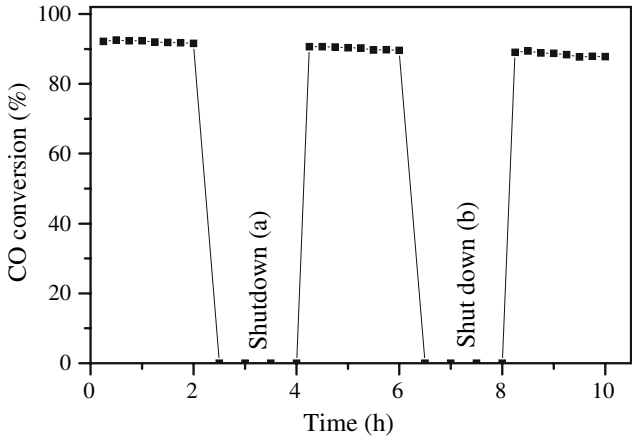

Fig. 8 Startup–shutdown cycles test of Pt–3Na/TiO_2 sample. Shutdown (a), H_2O + CO were removed when the temperature was cooled to room temperature; shutdown (b), only H_2O was removed when the temperature was cooled down to room temperature. Reaction conditions: 70% H_2, 30%, H_2O:CO = 5:1, GHSV = 7.0×10^4 cm^3/g-cat h (H_2O not included)

4 Conclusions

By controlling the amount of Na addition using a co-impregnation method, significant improvement in activity and stability of Pt/TiO_2 catalysts has been achieved compared to Pt/TiO_2, Pt/CeO_2 and Pt–1Re/TiO_2 catalysts. The optimal Na loading is 3 wt%. The catalyst is very stable when the reaction temperature is higher than 250 °C. The deactivation of Pt–3Na/TiO_2 catalyst at lower reaction temperatures (<250 °C) can be fully recovered when the reaction temperature is increased to higher than 250 °C. TEM observations show that addition of Na inhibits Pt sintering, possibly through the interactions of Pt–NaO_x–TiO_2. This catalyst is a promising single stage WGS catalyst for small scale hydrogen production applications. These results can be extended to addition of the proper amount of other alkali metals to improve the activity and stability of Pt/TiO_2 catalysts for the WGS reaction. Further studies of the reaction rate in the presence of different ratios of reactants and products with appropriate characterizations will clarify the role Na addition on Pt–NaO_x–TiO_2 structure as well as the effects on surface intermediates.

Acknowledgement Support from SEMGREEN, LP is greatly appreciated. Helpful discussions with Dr. C. T. Adams are appreciated.

References

1. Ladebeck JR, Wagner JP (2003) In: Vielstich W, Lamm A, Gasteiger HA (eds) Handbook of fuel cell-fundamentals, technology and applications, vol 3. John Willey & Sons, Ltd., Chichester, p 190
2. Bunluesion T, Gorte RJ, Graham GW (1998) Appl Catal B 15:107
3. Jacobs G, Graham UM, Chenu E, Patterson PM, Dozier A, Davis BH (2005) J Catal 229:499
4. Meunier FC, Tibiletti D, Goguet A, Shekhman S, Hardacre C, Burch R (2007) Catal Today 126:143
5. Hilaire S, Wang X, Luo T, Gorte RJ, Wagner J (2004) Appl Catal A 258:271
6. Zalc JM, Sokolovskii V, Löffler DG (2002) J Catal 206:169
7. Liu X, Ruettinger W, Xu X, Farrauto R (2005) Appl Catal B 56:69
8. Ruettinger W, Liu X, Farrauto RJ (2006) Appl Catal B 65:135
9. Deng WL, Flytzani-Stephanopoulos M (2006) Angew Chem Int Ed 45:2285
10. Azzam KG, Babich IV, Seshan K, Lefferts L (2007) J Catal 251:163
11. Pigos JM, Brooks CJ, Jacobs G, Davis BH (2007) Appl Catal A 319:47
12. Panagiotopoulou P, Kondarides DI (2004) J Catal 225:327
13. Panagiotopoulou P, Christodoulakis A, Kondarides DI, Boghosian S (2006) J Catal 240:114
14. Iida H, Igarashi A (2006) Appl Catal A 298:152
15. Sato Y, Terada K, Hasegawa S, Miyao T, Naito S (2005) Appl Catal A 296:80
16. Sato Y, Terada K, Soma Y, Miyao T, Naito S (2006) Catal Commun 7:91
17. Iida H, Igarashi A (2006) Appl Catal A 303:48
18. Li Y, Fu Q, Flytzani-Stephanopoulos M (2000) Appl Catal B 27:179
19. Jacobs G, Patterson PM, Williams L, Sparks D, Davis BH (2004) Catal Lett 96:97
20. Phatak AA, Koryabkina N, Rai S, Ratts JL, Ruettinger W, Farrauto RJ, Blau GE, Degass WN, Ribeiro FH (2007) Catal Today 123:224
21. Farrauto RJ, Liu Y, Ruettinger W, IIinich O, Shore L, Giroux T (2007) Catal Rev Sci Eng 49:141
22. Evin HN, Jacobs G, Ruiz-Martinez J, Thomas GA, Davis BH (2008) Catal Lett 120:166